# Translation initiation factors and active sites of protein synthesis co-localise at the leading edge of migrating MRC5 fibroblasts

Mark Willett, Michele Brocard, Alexandre Davide, Simon Morley

# Translation initiation factors and active sites of protein synthesis co-localise at the leading edge of migrating MRC5 fibroblasts

Mark Willett[1], Michele Brocard[1], Alexandre David [2], and Simon J. Morley[1*]

[1]Department of Biochemistry, School of Life Sciences, University of Sussex, Brighton BN1 9QG, UK.
[2] Laboratory of Viral Diseases, NIAID, NIH, Bethesda, MD 20892, USA

[*]corresponding author

Tel (01273) 678544
FAX (01273) 678433

Email: s.j.morley@sussex.ac.uk

Biochemical Journal Immediate Publication. Published on 04 May 2011 as manuscript BJ20110435

**Abstract**

Cell migration is a highly controlled, essential cellular process often dys-regulated in tumour cells, dynamically controlled by the architecture of the cell. Studies involving cellular fractionation and microarray profiling have previously identified functionally distinct mRNA populations specific to cellular organelles and architectural compartments. However, the interaction between the translational machinery *per se* and cellular structures is relatively unexplored. To help understand the role for the compartmentalisation and localised protein synthesis in cell migration, we have used scanning confocal microscopy, immunofluorescence and a novel ribopuromycylation method to visualise translating ribosomes. Here we show that initiation factors (eIFs) localise to the leading edge of migrating MRC5 fibroblasts in a process dependent on trans-Golgi network (TGN) to plasma membrane vesicle transport. Here we show that eIF4E and eIF4GI are associated with the Golgi apparatus and membrane microdomains and that a proportion of these proteins co-localise to sites of active translation at the leading edge of migrating cells.

**Key words**: translation initiation factor, localisation, Golgi apparatus, membrane microdomains.

**Abbreviations**: eIF, eukaryotic initiation factor; $m^7$GTP, 7-methyl guanosine triphosphate; SDS, sodium dodecyl sulphate; PVDF, polyvinylidine difluoride; PAGE, polyacrylamide gel electrophoresis; TCA, trichloroacetic acid; BFA, brefeldin A; FRET, Fluorescence Resonance Energy Transfer (FRET); rp, ribosomal protein.

**Acknowledgements**: we would like to thank Jonathan W. Yewdell (Laboratory of Viral Diseases, NIAID, NIH, Bethesda, MD 20892, USA) for advice and reagents used in this work. This work was supported by a grant from the BBSRC (UK).

Biochemical Journal Immediate Publication. Published on 04 May 2011 as manuscript BJ20110435



## Introduction

Cell migration is an essential process in development, morphogenesis [1] and angiogenesis [2]. Cells may move singly allowing the correct positioning in tissues during morphogenesis, or during the metastatic formation of secondary tumours in cancer. Alternatively, if cell-cell junctions are retained, collective polarity and a 'supracellular' cytoskeletal organisation is maintained, thereby allowing cells to move in 'sheets' for larger scale tissue remodelling during morphogenesis. Uncontrolled cell migration can lead to metastasis [3], tumour vascularisation [4], developmental defects [1], and atherosclerosis [5], events possibly reflecting dys-regulation of localised protein synthesis [6].

Protein synthesis is carried out in three stages (initiation, elongation and termination), with the initiation stage of translation generally accepted as a major site of regulation of gene expression [7-9]. This pivotal role reflects the regulated binding of mRNA to the ribosome, facilitated by the assembly of initiation factors into a multi-protein complex known as eIF4F (eIF4E, eIF4A, eIF4G) which is often unregulated in tumour cells [10]. In turn, the activity of this complex is regulated by both phosphorylation and the inherent structural properties of the recruited mRNA [9]. The formation of the eIF4F complex reflects the regulated availability of eIF4E to participate in initiation, a process controlled by a number of general and mRNA-specific regulatory proteins. Using a conserved motif, 4E-binding proteins (4E-BPs) compete with eIF4G for a common surface on eIF4E and inhibit eIF4F assembly. The localised association of 4E-BPs with eIF4E is acutely modulated by multi-site phosphorylation dependent upon mTORC1 signalling [7-9], effectively integrating signals from mitogens and nutrients with the translational apparatus [11-13].

Spatial localisation of mRNA can effectively regulate translation, facilitating the enrichment of proteins at their sites of function while additionally ensuring that proteins are expressed at appropriate local concentrations in proximity their cognate binding partners [14]. Indeed, the presence of β-actin mRNA, polyribosomes, and poly(A) binding protein (PABP) on cell protrusions suggests that specifically localised mRNA translation may be involved in the determination of the polarity of migrating cells, filopodia or pseudopodia [15-19]. Microarray profiling following cellular fractionation has identified functionally distinct mRNA populations specific to cellular organelles and compartments, including mitochondria, the mitotic apparatus, endoplasmic reticulum, neuronal dendrites and pseudopodia [20](reviewed in [21]). Differential compartmentalisation is often established by the incorporation of mRNA into large translationally silenced ribonucleoprotein complexes (mRNPs), which are then actively transported along microtubule or actin filaments; following transportation, the mRNA is activated, resulting in localised protein expression [22,23]. This asymmetric mRNA localisation is essential for a number of processes, including body axes formation in developing metazoans [14], synaptic plasticity [24], somatic and germline cell polarity [25]. mRNPs association with the cytoskeleton requires complex formation with motor proteins [22] including, myosin motor proteins which shuttle along actin microfilaments and dyneins and kinesins which shuttle cargo along microtubule networks [26]. Dedicated RNA-binding proteins, such as zipcode binding protein 1 (ZBP1) can be required, interacting with specific target mRNA sequences (zipcode elements) to form functional RNPs. Indeed, ZBP1 is important for the localised translational regulation of β-actin mRNA [18,27], maintaining translational repression during transport with its subsequent phosphorylation and release facilitating activation at the leading edge of the cell [18,27,28].

Traditionally, the compartmentalisation of ribosomes is thought to involve two pools: one associated with the Endoplasmic Reticulum (ER), where cells are provided with the means to facilitate the localised translation of luminal, secretory and trans-membrane proteins and a pool in which cytosolic proteins are synthesised [29]. However, cytosolic proteins are not only expressed on the ER, as ER-associated ribosomes translate a significant proportion of mRNAs encoding cytosolic proteins more efficiently than unbound ribosomes [29,30]. Surprisingly, the interactions between translation initiation factors, localised mRNAs and active sites of translation in the cell is relatively unexplored; although PABP is present with many localised mRNAs, whether they are translated at all and how the ribosomes interact with such target mRNAs to allow for localised protein expression has not been addressed.

To gain insight into the possible role for the compartmentalisation of the active translation machinery in cell migration, we have used scanning confocal microscopy and immunofluorescence studies coupled with a novel method of visualising actively translating ribosomes to monitor the co-localisation of initiation factors and ribosomes in transformed and non-transformed, migrating MRC-5 fibroblasts in 2D culture. Here we show that eIF4E and eIF4GI are associated with the Golgi apparatus and membrane microdomains and that a proportion of these proteins co-localise to sites of active translation at the leading edge of migrating cells.

**Experimental**

**Cell culture;** MRC5 cells were routinely cultured in MEM (Invitrogen, UK) supplemented with 10% (v/v) foetal bovine serum (Labtech, UK) in a humidified atmosphere containing 5% $CO_2$. **Immunocytochemistry;** Coverslips were coated 25 µg/ml bovine fibronectin (Sigma, UK) in PBS, incubated for 1 h then aspirated. For migration assays, $5 \times 10^4$ cells were seeded onto each 22 mm fibronectin coated coverslip and allowed to grow for 24 h. For cell spreading assays, cells were detached from their substrate with trypsin, washed, and held in suspension in a shaker in complete tissue culture medium for a recovery time of 45 minutes. $5 \times 10^4$ cells were then seeded onto each 22 mm coverslip, and the cells were recovered for fixation and staining at predetermined time points. Cells were then washed once in 1 ml PBS at 37 °C, then fixed in 4% paraformaldehyde in PBS for 20 min and permeabilised with 0.1% (v/v) Triton X-100/PBS for 5 min prior to staining. Following fixation and permeabilisation, non-specific binding was blocked by adding 3% (w/v) BSA in PBS for a minimum of 20 minutes at room temperature. Cells were incubated in the primary antibody solution for 1 hour, washed extensively and then incubated with the appropriate secondary antibody for 1 hour. Golgi vesicles were visualised using NBD $C_6$-ceramide complexed to BSA (Invitrogen, UK) and membrane microdomains visualised with BODIPY-FL-$C_5$ ceramide (Invitrogen, UK), respectively, during the second antibody incubation step. Following further extensive washing, nuclei were stained with DAPI for 5 minutes. After a further two washes, coverslips were mounted on microscope slides with Mowiol mounting solution (0.2 M Tris pH 8.5, 33% (w/v) glycerol, 13% (w/v) Mowiol, 2.5% (w/v) 1,4-diazobicyol [2,2,2]-octane (DABCO)) and sealed with clear nail polish. Images were collected on a Zeiss Axiovert LSM510 scanning confocal microscope using a 63× objective. Single stain, bleed-though controls and antibody cross-reaction controls were prepared for each sample (data not shown). Cell diameter, ROI intensity values for FRET experiments, Costes' approach Pearsons correlation coefficients and *p*-values were calculated using MBF ImageJ (http://www.macbiophotonics.ca/).

**Puromycylation assay by immunofluorescence;** for the puromycylation assay, 22 $mm^2$ glass coverslips were coated with fibronectin (20 μg/ml) for 1 hour at room temperature. MRC-5 cells (5 x $10^5$) were then seeded onto each coverslip and cultured at $37^0$C for 24 hours. Cells were then incubated with 91 μM puromycin and 208 μM emetine (Sigma, UK) for 5 minutes. The coverslips were then washed twice in ice cold PBS supplemented with 355 μM cycloheximide and then incubated on ice in PBS containing 0.00375% (w/v) saponin, for 30 seconds to pre-permeabilise the cells and reduce background staining, followed by rapid washing in ice cold PBS. Cells were then fixed by incubation for 15 minutes in 4% Paraformaldehyde/PBS (Electron Microscopy Supplies, UK). Following fixation, coverslips were washed three times in PBS and cells permeabilised for 5 minutes as above, followed by three further washes in PBS. Following pre-blocking using 2% gelatin (Sigma, UK) for 20 minutes, cells were incubated for 1 hour at room temperature with mouse anti-puromycin-specific mAb in 2% gelatin/PBS. After washing three times with PBS, coverslips were incubated with goat anti-mouse A488 (Molecular Probes, UK) for 1 hour at room temperature and then processed as described above.

**Preparation of cell extracts;** Cells were isolated in a cooled centrifuge and washed with 0.5 ml ice-cold PBS containing 40 mM β-glycerophosphate and 2 mM benzamidine. Pellets were resuspended in 200 μl ice-cold Buffer A [20 mM MOPS/KOH, pH 7.2, 10%(v/v) glycerol, 20 mM sodium fluoride, 1 μM microcystin LR, 75 mM KCl, 2 mM $MgCl_2$, 2mM benzamidine, 2 mM sodium orthovanadate, complete protease inhibitor mix (-EDTA (Roche)) and lysed by vortexing following the addition of 0.5% (v/v) Igepal and 0.5% (v/v) deoxycholate. Cell debris was removed by centrifugation in a microfuge for 5 minutes at 4°C and the resultant supernatants frozen in liquid $N_2$.

**Crude fractionation;** Cells were harvested by scraping, washed and resuspended in hypotonic homogenisation buffer [10 mM MOPS/KOH pH 7.3, 10 mM potassium acetate, 1.5 mM magnesium acetate, protease inhibitor cocktail (Roche, UK)] and disrupted using shear forces. Following normalisation of the potassium concentration to 50 mM, the cells were centrifuged at 10,000 x *g* and the supernatant collected as the cytosolic fraction. The remaining pellet was then resuspended and lysed in an equal volume of buffer [20 mM MOPS/KOH pH 7.2, 25 mM KCl, 2 mM $MgCl_2$, 2 mM benzamidine, 2 mM EGTA, 0.1 mM GTP, 0.5 mM DTT, 10 % (v/v) glycerol and protease inhibitor (Roche, UK). Following a further centrifugation at 10,000 x *g*, the supernatant was collected as the detergent extracted fraction. The remaining pellet was then resuspended and lysed in an equal volume of 6 M urea to recover remaining detergent insoluble proteins.

**m7GTP-Sepharose affinity isolation of eIF4E and associated factors;** For the isolation of eIF4E and associated proteins, cell extracts of equal protein concentration were subjected to $m^7$GTP-Sepharose chromatography and the resin was washed twice with Buffer B [20 mM MOPS/KOH pH 7.4, 75 mM KCl, 2 mM $MgCl_2$, 1 μM microcystin LR, 10 mM NaF, 2 mM benzamidine, 7 mM 2-mercaptoethanol, 0.1 mM GTP], as described [31-34]. Recovered protein was eluted directly into sample buffer for SDS-PAGE [31-33].

**Iodixanol gradients;** The manufacturers published protocol was used with some minor modifications. Briefly, cells were washed twice in PBS and then once in Homogenisation medium: [0.25 M sucrose, 1 mM EDTA 10 mM HEPES/NaOH, pH 7.4] cells were then resuspended in 0.5 ml Homogenisation medium and disrupted by Dounce homogenisation. The homogenate was then centrifuged at 2000 x *g* for 10 min and the supernatant was loaded onto continuous 5 ml 2-22% Iodixanol gradients (Axis-Shield, UK) [Diluent: 0.25 M sucrose, 6

mM EDTA, 60 mM HEPES/NaOH, pH 7.4] and centrifuged at 150,000 x *g* for 1.5 hours. Gradients were then passed through a fraction collector (Brandel, USA) and 0.5 ml fractions were collected. Proteins were resolved using SDS-PAGE and western blotting.

**Antisera;** Rabbit antibodies included anti-rpS3, rpL7a, rpS6 and 4E-BP1 were from Cell Signalling Technology. In-house rabbit antisera were raised against: a C-terminal peptide of eIF4GI (RTPATKRSFSKEVEERSR; amino acids 1179-1206 and used at 1 in 200 dilution); eIF4E peptide (TATKSGSTTKNRFVV; amino acids 203–217, used at a 1 in 50 dilution). These rabbit antisera were immunopurified from crude serum by affinity chromatography with the corresponding peptide using the SulfoLink kit (Perbio Science, UK) according to the manufacturer's instructions. These eIF4G and eIF4E antisera have been used in previous immunofluorescence studies [19,35]. Mouse monoclonal antibodies included anti-β-tubulin clone DM 1A (both FITC conjugate and unconjugated; Sigma, UK) anti-actin (Sigma, UK) and anti-golgin97 CDF4 (Molecular Probes, UK) [36]. Secondary antibodies used were AlexaFluor 488 Goat anti-mouse IgG, AlexaFluor 555 Goat anti-rabbit IgG and AlexaFluor 647 Goat anti-mouse IgG (Molecular Probes, UK). For the puromycylation assay (see below), mouse PMY-specific mAb (clone 12D10) was used.

**Fluorescence Energy Transfer (FRET);** FRET was determined using a Zeiss LSM510 Meta confocal microscope mounted on a Zeiss Axiovert chassis. Immunofluorescence FRET using the Alexa 488/Alexa 555 FRET pair was chosen (Molecular Probes, UK), giving a Förster radius of ~70 Å. Acceptor photobleaching FRET was used, a method of measuring FRET developed for laser scanning confocal microscopy [37]. Following collection of an initial multi-channel image using standard parameters, energy transfer was detected as an increase in donor fluorescence (Alexa 488) after complete photobleaching of the acceptor molecules (Alexa 555) by multiple passes with a 543 nm laser within defined a ROI. A second multi-channel image was collected, and the amount of energy transfer was calculated as the percentage increase mean pixel intensity within the defined ROI between two images in the Alexa 488 donor channel after acceptor fluorophore photobleaching. This process was repeated on multiple cells and the mean and standard deviation values were calculated.

## Results

To directly address the interactions between components of the active translational machinery and intracellular structures, we initially used a crude fractionation method where cell-free extracts, enriched for cytosolic and soluble proteins were separated from detergent soluble and membranous fractions using detergents and low speed centrifugation. Detergent-insoluble fractions were collected in buffer containing 6M urea and the distribution of eIF4E and selected marker proteins were visualised SDS-PAGE and Western blotting. As shown in Fig.1A, the majority of total eIF4E was cytosolic (lanes 1 and 2); detergent was required to recover the remaining eIF4E (lanes 3 and 4), suggesting that it was bound to sub-cellular components. The latter population of eIF4E co-fractionated with the intracellular membrane markers, PDI and calnexin (lanes 3 and 4). Similarly, β-tubulin (Fig.1A, lanes 3 and 4), eIF4B and PABP (Fig.1B, lanes 1-4) were recovered in both the cytosolic (lanes 1 and 2) and a detergent-soluble fractions (lanes 3 and 4). There was no evidence that eIF4E co-fractionates with detergent insoluble, polymerised actin or with vimentin, which is entirely detergent-insoluble (lanes 5 and 6). In contrast, eIF4GI, eIF4A, as well the p170 and p110 subunits of eIF3 [7] were present in the insoluble fraction (lanes 5 and 6). The p47 and p35 subunits of eIF3, together with eIF2α appeared to be largely soluble (lanes 1 and 2). Using densitometry

of data from a representative experiment, we were able to determine that approximately 25 % of eIF4E exists in a detergent soluble fraction (Fig.1C).

To further investigate the co fractionation of eIF4E with intracellular membranes, laser scanning confocal microscopy was used in combination with immunocytochemistry, enabling a comparison to be made between the staining patters for eIF4E, the Golgi apparatus, membrane microdomains and the ER. To visualise the Golgi apparatus, we used golgin97 and NBD-$C_6$-ceramide; for the ER we used calnexin and for the membrane microdomains, BODIPY-FL-$C_5$ ceramide coupled to BSA. In addition, to quantify the degree of localisation, the Pearsons co-localisation coefficient (*R(obs)*) was calculated, and this was statistically confirmed using Costes' approach [38]. This allows for the calculation of Pearson's correlation coefficient *R(obs*), which also accounts for any random overlay of pixels by generating the mean correlation coefficient *R(rand)* between *n* images which have identical average pixel intensity to the original images, but a random distribution of pixels. In theory, an *R(obs)* of +1 would represent a perfect pixel correlation between two channels in an image. Although many values we obtained did not reach this theoretical maximal value, the fact that most data show a low value for *R(rand)* suggests that many co-localisations we observed in this study could be significant. As shown in Figs.2A and 2B, we observed a significant co-staining between eIF4E and the Golgi apparatus stained with $C_6$-ceramide (*R(obs)* of 0.617 with a *p*-value of 100 %). Using BODIPY-FL-$C_5$ ceramide, we have shown that eIF4E is present in specific membrane microdomains, present in the lamellipodia and perinucluclear regions of migrating cells (Fig.2C-E). These membrane microdomains present in lamellipodia (Figs.2D and E) were analysed further by applying an intensity vector across one of the co-stained vesicles. With the lamellipodia (Fig.2D), the resulting profile showed similar intensities for both stains across the vector (lower panel; *R(obs)* of 0.621 with a *p*-value of 100 %). We also observed $C_5$-ceramide and eIF4E-enriched vesicles that extended from the perinuclear area to the periphery of the cell (Fig.2E; *R(obs)* of 0.734 with a *p*-value of 100 %), suggesting that intracellular membrane transport may be involved in the transportation of the translational machinery. The finding that $C_5$-ceramide and eIF4E stains also co-localise in the lamellipodia of migrating cells, indicate that membrane microdomains may be responsible the lamellipodial localisation of eIF4E (Fig.2C). To compare the localisation of eIF4E with the ER and Golgi, we co-stained cells for eIF4E, calnexin, or golgin97, respectively. Fig.2F shows an incomplete overlap of Golgi/eIF4E and ER/eIF4E staining in migrating cells. A high-contrast LUT was applied to the images, and a region of interest was drawn around the calnexin and golgin-positive regions. When both ROI were combined it was found that they completely overlapped the eIF4E stain, suggesting that the majority of bound eIF4E is associated with the ER and Golgi in such migrating cells.

To confirm that eIF4E was present on the Golgi and ER, clarified cell extracts were resolved on continuous 2-20 % iodixanol gradients. Fractions were collected and recovered proteins were resolved using SDS-PAGE; Western blotting was used to probe for the Golgi marker golgin97, the ER marker, calnexin, eIF4E, eIF4GI and 4E-BP1 (Fig.3). eIF4E was seen to fractionate into two main pools; one co-fractionating with the majority of 4E-BP1 and eIF4GI in the hydrosol and light fractions (lanes 1 to 3), and one in the heavy fractions (lanes 5 to 7). Although they do not precisely co-fractionate, the light fractions also contained the Golgi marker, golgin97 (lanes 2 and 3), consistent with the localisation studies shown in Fig.3. The incomplete co-fractionation probably reflects the reported heterogeneity of vesicles in such cells [39, 40]. As eIF4E co-fractionated with calnexin in the heavy fractions (lanes 6 to 8), these data indicate that this pool of eIF4E is likely associated with the ER.

Translational control often mirrors the regulated binding of mRNA to the ribosome, facilitated by the assembly of initiation factors into the multi-protein eIF4F complex [7-9,11]. However, the relationship between the need for compartmentalised translation and how the protein synthesis machinery is localised is poorly understood. To investigate whether the Golgi or membrane microdomains are responsible for transporting a proportion of eIF4E to the lamellipodia of migrating cells, cells were enzymatically detached from their growth surface, held in suspension, and then allowed to spread for 45 minutes until they formed lamellipodia-like structures around their periphery. As shown in Fig.4A, eIF4E was localised to the leading edge of the spreading cell (upper panel). Whilst in suspension, cells were also incubated in the presence of brefeldin-A (BFA) to inhibit Golgi to plasma membrane transport. BFA (lower panels) prevented the recovery of eIF4E at the leading edge on cell spreading. Quantification of these data (Fig.4B) indicated that BFA caused a 75 % reduction in the incidence of eIF4E localised to the cells periphery ($p$= <0.01%), without directly affecting cell spreading (Fig.4C). These data implicate the Golgi apparatus in the localisation of eIF4E. To investigate the requirement for active translation in this process, cells in suspension were incubated with the mTORC1 inhibitor, RAD001 [41] the mTORC1 and mTORC2 inhibitor, Torin 1 [42], the ternary complex inhibitor, NSC119893 [43], or the eIF4G complex assembly inhibitor, 4E-G1 [44]. Although there were no effects on cell spreading for any treatment, inhibition of eIF4E/eIF4G complex formation with 4E-G1 resulted in reduced eIF4F complex levels (data not shown) and a 50% reduction in the incidence of eIF4E localised to the cells periphery (Figs.4B/C; $p$= <0.05%). This was not observed following treatment of cells with Torin 1, RAD001 or NSC119893 (Fig.4B). These data support the observation that Golgi-lamellipodium localised *de novo* protein synthesis is not essential for initiating the establishment of lamellipodia [45].

To understand how these data relate to the apparent co-isolation of eIF4E with tubulin (Fig.1), we used spreading MRC5 cells and employed a combination of confocal microscopy and co-isolation of protein complexes using mRNA cap affinity chromatography. Fig.5A shows that although the eIF4E stain did not overlap the stain for microtubules, the eIF4E-enriched vesicles line-up with, and decorate microtubules (lower panel). Fig.5B shows that this association extends into the lamellipodia with both proteins enriched in the same structures on the leading edge of the cell. To clarify whether eIF4E makes a close or direct association with microtubules in migrating cells, we employed acceptor photobleach Fluorescence Resonance Energy Transfer (FRET). Fig.5C shows that following bleach of the eIF4E signal, on average, the pixel intensity for the tubulin stain increased by 31% (+/-13%, n=3) in the microtubule organising centre (MTOC), consistent with an inter-fluorophore separation of 8-9 nm for the population of eIF4E associated with the MTOC (Fig.5D). Similar effects were seen with individual lamellipodium but no increase in donor FRET was observed on microtubules transiting the lamellum (Fig.5C). To investigate whether the cap binding complex, eIF4F associates with microtubules, extracts were recovered for suspension cells (Sus), cells that had been left to spread for 45 minutes (Spr) and growing cells (Unt). eIF4E and associated proteins were then recovered using $m^7$GTP-Sepharose chromatography and visualised by Western blotting (Fig.5E). Surprisingly, both tubulin and actin were recovered in association with eIF4E in growing cells and those held in suspension (lane 6 vs. lane 4). In contrast, even though eIF4G and PABP were recovered in the eIF4F complex, actin and tubulin were not co-isolated with eIF4E in cells that were actively spreading (lane 5 vs. lane 6).

The presence of a significant population of ribosomes on the leading edge of migrating fibroblast-like cells was first established by scanning electron microscopy [15]. Further work

showed that mRNA localised to focal adhesions [46], whilst PABP localised to the dense ER and to the leading edge of migrating cells, associating with paxillin [47]. Ablation of the PABP/ER interaction impaired migration and spreading of cells on a fibronectin substrate indicating that localised protein synthesis may have a role in cell motility. These data led us to utilise scanning confocal microscopy to visualise the localisation of other components of the translational machinery in relation to intracellular membranes in spreading cells. Staining patterns from antisera raised against eIF4GI, eIF4E, 4E-BP1, 40S ribosomal subunits (ribosomal protein (rp)S3, rpS6), and 60S ribosomes (rpL7a) were compared to those obtained for the ER, Golgi and the microtubule cytoskeleton. Costes' method was used to define the degree of co-localisation (in ROIs) in the perinuclear region and at the lamellopodia. These data (Fig.6A-F) clearly show that eIF4E co-localises with eIF4G in both the perinuclear area and on lamellipodia (Panel A), with a high R(obs); there is less apparent localised interaction between eIF4E and 4E-BP1 at the leading edge of the cell, suggestive of localised, active translation in this compartment (Panel B). Ribosomal subunits (small and large) co-localise with the membrane microdomain marker $C_5$-ceramide (Panels C and F), β-tubulin (Panel E) and the ER marker, calnexin (Panel D) in both the perinuclear and lamellipodia regions. We have also investigated the co-localisation of rpS6 and paxillin in lamellipodia (Fig.6G). These data show that at the level of the focal adhesion complex attaching to the cell surface, there is little co-localisation of paxillin and rps6 (quantified in the lower panel). However, above 0.5-1.5 μm from the attachment surface, these proteins are found in the same compartment. In total, these data suggest that active initiation of translation as well as translational regulation may be taking place in these structures.

To directly visualise localised sites of active protein synthesis in live cells, we utilised a novel technique employing puromycin and confocal microscopy. Puromycin mimics tyrosine-tRNA and enters the A site of eukaryotic ribosomes where it is incorporated into nascent chains, terminating translation. Using anti-puromycin polyclonal Abs, Eggers *et al.,* [48] detected and captured puromycylated nascent chains from permeabilised cells. This method has recently been adapted and modified by the Yewdell lab to visualise sites of active translation in Vaccinia virus infected HeLa cells. As shown in Fig.7A, puromycin-positive nascent polypeptide chains were observed at the leading edge of migrating cells; staining with puromycin was prevented by salt shocking the cells, conditions previously shown to strongly inhibit the initiation of protein synthesis [49]. Co-staining patterns showed that active sites of translation co-localised with eIF4E and rpS6 (both in their less and more phosphorylated states) in both the perinuclear area and on lamellipodia at the leading edge of MRC5 cells (Fig.7B). In agreement with the data presented in Fig.6, these sites also contained eIF4GI. As mTORC1 signalling has a central role in translation control, we have also investigated the localisation of mTOR and Raptor to these sites of active translation [8,9]. Fig.7B shows that components of the mTORC1 complex (mTOR/raptor) co-stained with puromycin-labelled nascent chains, consistent with these reflecting sites of on-going translation [7,12,13].

## Discussion

In the work described here we have started an investigation using confocal microscopy to directly address the interactions between components of the active translational machinery and intracellular structures. In agreement with our previous work [35], crude fractionation of extracts showed that approximately 25 % of cytoplasmic eIF4E exists in a detergent soluble fraction (Fig.1C). We now show that this population of eIF4E co-fractionates with microtubules and intracellular membranes, but not with polymerised actin or with vimentin. FRET analysis also supports this observation, suggesting that although tubulin and eIF4E are in close proximity in the MTOC region, they might not be directly interacting (Fig.5). The recovery of actin in association with eIF4E isolated by $m^7$GTP-Sepharose chromatography from migrating cells (Fig.5E) was surprising. This might be explained by recovery of actin protein-associated mRNAs via the cap structure or cross-linking of the microtubule and microfilament cytoskeletons by proteins such as plectin [50], allowing for the recovery of actin with tubulin/eIF4E on the resin. Interestingly, in the same experiment (Fig.5), the co-isolation of eIF4E with actin or tubulin was not observed during cell attachment and spreading assays. Cell spreading is a state in which eIF4E is most clearly associated with intracellular membranes, whereas with cell migration, the Golgi is highly polarised towards the plasma membrane [45, 51-54]. These data imply that (with the exception of initiation on ER-associated ribosomes) eIF4E may have specific physiological roles that require its localisation or anchorage to particular membranous loci. Association between initiation factors and the dynamic and polarised Golgi apparatus of migrating cells [54] may be involved in localised translation which could modulate or enhance cell polarisation. Alternatively, these vesicles might function as an intracellular transport medium to move the translational machinery to the leading edge of the polarised cell to promote migration. Such a transport mechanism might explain why in monolayer cells subjected to “scratch” wounding assays, there is a requirement for the Golgi to be polarised towards the leading edge of cells migrating to close the “wound” [51,54-56]. The identity of mRNAs translated or transported in such a manner still needs to be determined. As described for Cdc42 [54], it will be interesting to determine whether proteins such as Arf6 bind directly to eIF4E and link cell polarity with localised translation.

We have clearly seen an association between growth factor-regulated initiation factors, the Golgi apparatus and membrane microdomains in spreading cells (Figs.2/3). In transformed MRC5 fibroblasts, eIF4E-enriched vesicles derived from the Golgi line-up with and decorate microtubules, highly consistent with that of large pleomorphic carriers (LPCs), which align with, and are dependent upon microtubules for transportation [56]. Fig.5B shows that this association extends into the lamellipodia with both proteins enriched in the same structures on the leading edge of the cell. This might reflect an increased association of eIF4E-bound mRNAs with intracellular membranes, perhaps as a large-scale mechanism to rapidly redeploy the translational machinery to areas of the cell in which actively translation is required. Ceramide, golgin97 and eIF4E-enriched LPCs were often observed extending to the lamellipodium, and always polarised towards the leading edge of freely migrating cells. Such membrane microdomains, along with the Golgi apparatus, comprise highly dynamic cytoskeleton-linked networks which facilitate intracellular transport of small round vesicles [57] and LPCs [58]. Such localisation of eIF4E to vesicles was unexpected, but is consistent with the intracellular localisation of 4E-BP1/eIF4E to effectors such as mTOR, TSC2, and Rheb in mTORC1 signalling [12,13] to membrane microdomains [40,59-62]. However, both inhibitors of mTORC1 and protein synthesis in general failed to have any observable effect on cell

spreading or the localisation of eIF4E (Fig.3). These data suggest that whilst Golgi-lamellipodium localised *de novo* protein synthesis is not essential for initiating the establishment of lamellipodia [45], it may still be important in modulating cell migration. Indeed, Fig.6 shows that a number of other translation initiation factors and ribosomal subunits co-localise with eIF4E present on the Golgi apparatus and the lamellipodia of migrating cells, including the eIF4F scaffold protein, eIF4GI and to a lesser extent, 4E-BP1. These data are suggestive of localised, active translation in this compartment. Fig.6G shows that active initiation of translation [20] as well as translational regulation may be taking place 0.5-1.5 μm above the attachment surface.

To directly visualise localised sites of active protein synthesis, we utilised a novel puromycylation assay coupled with confocal microscopy to co-stain nascent polypeptide chains and initiation factors. Fig.7 shows that active sites of translation co-localised with eIF4E, rpS6, eIF4G and components of the mTORC1 complex (mTOR/raptor). These data are consistent with the binding of mTORC1 to the pre-initiation complex on polysomes [63] and its functional association with both the ER and Golgi [59,60,64-66]. Taken together, our study suggests that ER/Golgi association of mTOR/raptor may facilitate not only the activity of mTORC1 [12,13,67] but also facilitate the transport of initiation factors to the leading edge of the migrating cell and promote localised translation. We are currently trying to identify which mRNAs are preferentially utilised at the leading edge of the cell. Candidates mRNAs could include β-actin mRNA, found in cell protrusions and involved in filopodia formation [17-19,27]; Cdc42, Rab13,and molecular motors which are involved in cell motility and polarity or mRNAs encoding initiation factor polypeptides [20,54].

## Figure legends

**Fig 1. eIF4E co-fractionates with microtubules and intracellular membranes**

Cells were harvested and lysed as described in the Experimental section, generating the cytosolic fraction (lanes 1 and 2). The resulting pellet was resuspended and lysed in buffer containing 0.5 % (v/v) igepal and 0.5 % (v/v) deoxycholate, and this lysate was centrifuged at 10,000 x *g,* generating the detergent-extracted fraction (lanes 3 and 4). The remaining pellet was resuspended in 6 M urea and centrifuged at 10,000 x *g* to isolate the detergent insoluble supernatant (lanes 5 and 6). No nuclear lysis was observed (data not shown). Fractions were then visualised by SDS-PAGE and Western blotting using the antisera shown.

**Panel A.** Western blots were probed for eIF4E, membrane markers (calnexin and PDI) and cytoskeleton markers, as indicated.

**Panel B.** Western blots were probed for eIF4A, PABP, eIF4B, eIF4GI, eIF3 and eIF2$\alpha$

**Panel C.** The relative enrichment of eIF4E in each fraction was determined using densitometry of the Western blots shown in Panel A.

**Fig 2. eIF4E co-stains with the Golgi apparatus, the ER and membrane microdomains in the perinuclear region and lamellipodia**

Cells were fixed and prepared for confocal microscopy as described in the Experimental section. The subcellular distribution of eIF4E was investigated using direct immunocytochemistry, using an eIF4E polyclonal IgG-Alexa 555 conjugate. The Golgi apparatus was visualised using the Golgi-enriched $C_6$-ceramide sphingolipid, membrane microdomains using BODIPY-$C_5$ ceramide conjugated to BSA, or by indirect immunocytochemistry with monoclonal antibodies raised against the Golgi-enriched protein, golgin97. The ER was visualised using indirect immunocytochemistry using antisera raised against the ER-enriched protein, calnexin. Covariance between channels was measured using Coste's approach (see text for details).

**Panel A.** Fixed cells were co-stained with eIF4E and $C_6$-ceramide; individual images show the single staining for eIF4E or $C_6$-ceramide alone to visualised the Golgi apparatus**.**

**Panel B.** shows a merged image following co-staining of cells for eIF4E and $C_6$-ceramide.

**Panel C.** eIF4E was co-stained with $C_5$-ceramide and covariance between channels in the lamellipodium was investigated as in Panel A.

**Panel D.** eIF4E was co-stained with $C_5$-ceramide and covariance between channels in the perinuclear area was investigated using Coste's approach and vector profiling (inset).

**Panel E.** eIF4E was co-stained with $C_5$-ceramide and covariance between channels in the lamellum was investigated as in Panel A.

**Panel F.** eIF4E was co-stained with golgin97 and calnexin and a high-contrast LUT was applied to all channels. ROIs were traced around the areas of highest contrast in the calnexin and golgin97 channels (calnexin pseudo-coloured in red, golgin97 pseudo-coloured in green), these were then overlaid and compared with the eIF4E stain. Covariance between channels was measured using Coste's approach (see text for details).

**Fig 3. eIF4E co-fractionates with Golgi and ER membrane microdomains**

Cells were harvested by scraping, resuspended in hypotonic buffer and lysed by shear forces, as described in the Experimental section. Extracts were layered over 2-22% Iodixanol gradients and centrifuged at 150,000 x *g* for 1.5 hours to separate Golgi from ER vesicles. Fractions were collected as indicated (lanes 1-9; top to bottom, respectively) and the

distribution of proteins shown was visualised using SDS-PAGE and Western blotting. Calnexin and golgin97 were employed as markers of the ER and Golgi apparatus, respectively.

**Fig 4. Inhibition of intracellular vesicle trafficking abrogates the localisation of eIF4E to the periphery of spreading cells**
To induce spreading, cells were detached from their growth substrate and allowed to spread on fibronectin-coated coverslips for 30 minutes in the presence of absence of: the vesicle transport inhibitor, brefeldin-A (BFA); the eIF4F inhibitor, 4E-GI; the mTORC1 and 2 inhibitor, Torin1; the mTORC1 inhibitor, RAD001; or the ternary complex inhibitor, NSC119893. Cells were then fixed and prepared for confocal microscopy as described in the Experimental section. The subcellular distribution of eIF4E was investigated using direct immunocytochemistry with an eIF4E polyclonal IgG-Alexa 555 conjugate.
**Panel A.** Untreated cells (**upper panel**) and cells treated with brefeldin-A (**lower panel**) showing the effect of drug treatment on the microtubular network and on the re-localisation of eIF4E to the cell periphery (insets).
**Panel B.** 100 cells from each treatment were blind-scored for peripheral localisation of eIF4E during 30 minutes of spreading.
**Panel C.** 100 cells from each treatment were measured for their diameter following 30 minutes of spreading.

**Fig 5. eIF4E co-localises with the tubulin at the centrosome (MTOC) and the lamellipodium, but not in the lamellum**
Cells were fixed and prepared for scanning confocal microscopy, as described in the Experimental section. The subcellular distribution of eIF4E was investigated using direct immunocytochemistry with an eIF4E polyclonal IgG-Alexa 555 conjugate. Microtubules were visualised using a directly Alexa 488-conjugated monoclonal IgG.
**Panel A.** Distribution of eIF4E and microtubules in the lamellum (inset in lower panel).
**Panel B.** Distribution of eIF4E and microtubules in the lamellipodium (inset in lower panel).
**Panel C.** Acceptor photobleaching FRET of eIF4E and microtubules in the MTOC and lamellipodium. **Left panel**: Before photobleaching an ROI in the acceptor channel (eIF4E, 555 nm) with a 543 nm laser. **Right panel**: Post-photobleach intensity changes in the donor channel (β-tubulin, 488 nm), as indicated.
**Panel D.** Graph detailing predicted FRET efficiencies *vs* inter-fluorophore distance for the alexa 488/alexa 555 FRET pair.
**Panel E.** Cells were untreated (Unt), detached from their growth substrate and maintained in suspension (Sus) or allowed to spread on tissue culture dishes (Spr) for 45 minutes, as described in the Experimental section. Cells were then harvested and subjected to $m^7$GTP-Sepharose chromatography to isolate eIF4E and associated proteins. The recovery of initiation factors, actin and β-tubulin was then visualised using SDS-PAGE and Western blotting, as indicated.

**Fig 6. Co-localisation of ribosomes and initiation factors in relation to microtubules, intracellular membranes and lamellipodia in MRC5 cells**
**Panels A-F.** Migrating cells were fixed and stained as described in the Experimental section. The subcellular distribution of the initiation factors and ribosomal proteins indicated was

visualised using scanning confocal microscopy, as described. Covariance between channels was measured using Coste's approach (see text for details).
**Panel G.** Migrating cells were fixed and stained for rpS6 and paxillin, as described. Their distribution at different distances from the ventral surface of a lamellopodium was visualised using scanning confocal microscopy and z-stack analysis. Covariance between channels was measured using Coste's approach (see text for details) and is presented in graphical form.

**Fig.7. Puromycin-positive nascent polypeptide chains are present at the leading edge of migrating cells**
**Panel A.** Migrating cells, incubated in the absence or presence of 150 mM added NaCl for 30 minutes, were fixed and stained with anti-puromycin mAb, as described in the Experimental section and visualised using scanning confocal microscopy.
**Panel B.** Migrating cells were fixed and stained as described in the Experimental section. The subcellular distribution of initiation factors, ribosomal proteins, P-mTOR, Raptor and sites of active translation (using anti-puromycin mAb), were visualised using scanning confocal microscopy, as described. Covariance between channels was measured using Coste's approach (see text for details).

## References

1 Friedl, P. and Gilmour, D. (2009) Collective cell migration in morphogenesis, regeneration and cancer. Nat. Rev. Mol. Cell Biol. **10**, 445-457
2 Cai, W. J., Li, M. B., Wu, X. Q., Wu, S., Zhu, W., Chen, D., Luo, M. Y., Eitenmuller, I., Kampmann, A., Schaper, J. and Schaper, W. (2009) Activation of the integrins alpha 5 beta 1 and alpha v beta 3 and focal adhesion kinase (FAK) during arteriogenesis. Mol. Cell. Biochem. **322**, 161-169
3 Hall, A. (2009) The cytoskeleton and cancer. Cancer Metastasis Rev. **28**, 5-14
4 Winkler, F., Kienast, Y., Fuhrmann, M., Von Baumgarten, L., Burgold, S., Mitteregger, G., Kretzschmar, H. and Herms, J. (2009) Imaging Glioma Cell Invasion In Vivo Reveals Mechanisms of Dissemination and Peritumoral Angiogenesis. Glia. **57**, 1306-1315
5 Burtea, C., Laurent, S., Murariu, O., Rattat, D., Toubeau, G., Verbruggen, A., Vansthertem, D., Elst, L. V. and Muller, R. N. (2008) Molecular imaging of alpha(v)beta(3) integrin expression in atherosclerotic plaques with a mimetic of RGD peptide grafted to Gd-DTPA. Cardiovasc. Res. **78**, 148-157
6 Martin, K. C. and Ephrussi, A. (2009) mRNA Localization: Gene Expression in the Spatial Dimension. Cell. **136**, 719-730
7 Morley, S. J., Coldwell, M. J. and Clemens, M. J. (2005) Initiation factor modifications in the preapoptotic phase. Cell. Death. Diff. **12**, 571-584
8 Proud, C. (2008) mTOR signalling and human disease. J. Med. Genet. **45**, S33-S43
9 Sonenberg, N. and Hinnebusch, A. G. (2009) Regulation of Translation Initiation in Eukaryotes: Mechanisms and Biological Targets. Cell. **136**, 731-745
10 Wendel, H. G., Silva, R. L. A., Malina, A., Mills, J. R., Zhu, H., Ueda, T., Watanabe-Fukunaga, R., Fukunaga, R., Teruya-Feldstein, J., Pelletier, J. and Lowe, S. W. (2007) Dissecting eIF4E action in tumorigenesis. Genes Dev. **21**, 3232-3237
11 Jackson, R. J., Hellen, C. U. T. and Pestova, T. V. The mechanism of eukaryotic translation initiation and principles of its regulation. Nat. Rev. Mol. Cell Biol. **11**, 113-127
12 Sengupta, S., Peterson, T. R. and Sabatini, D. M. Regulation of the mTOR Complex 1 Pathway by Nutrients, Growth Factors, and Stress. Mol. Cell. **40**, 310-322
13 Zoncu, R., Efeyan, A. and Sabatini, D. M. mTOR: from growth signal integration to cancer, diabetes and ageing. Nat. Rev. Mol. Cell Biol. **12**, 21-35
14 St Johnston, D. (2005) Moving messages: The intracellular localization of mRNAs. Nat. Rev. Mol. Cell Biol. **6**, 363-375
15 Boyde, A. and Bailey, E. (1977) Observations on marginal ruffles of an established fibroblast-like cell line. Cell Tissue Res. **179**, 225-234
16 Woods, A. J., Kantidakis, T., Sabe, H., Critchley, D. R. and Norman, J. C. (2005) Interaction of paxillin with poly(A)-binding protein 1 and its role in focal adhesion turnover and cell migration. Mol. Cell. Biol. **25**, 3763-3773
17 Oleynikov, Y. and Singer, R. H. (2003) Real-time visualization of ZBP1 association with beta-actin mRNA during transcription and localization. Curr. Biol. **13**, 199-207
18 Huttelmaier, S., Zenklusen, D., Lederer, M., Dictenberg, J., Lorenz, M., Meng, X. H., Bassell, G. J., Condeelis, J. and Singer, R. H. (2005) Spatial regulation of beta-actin translation by Src-dependent phosphorylation of ZBP1. Nature. **438**, 512-515
19 Willett, M., Pollard, H. J., Vlasak, M. and Morley, S. J. (2010) Localisation of translation initiation factors to talin/beta3-integrin-enriched adhesion complexes in spreading and migrating mammalian cells. Biol Cell **102**, 265-76
20 Mili, S., Moissoglu, K. and Macara, I. G. (2008) Genome-wide screen reveals APC-associated RNAs enriched in cell protrusions. Nature. **453**, 115-119
21 Lécuyer, E., Yoshida, H. and Krause, H. M. (2009) Global implications of mRNA localization pathways in cellular organization. Curr. Opin. Cell Biol. **21**, 409-415
22 Vale, R. D. (2003) The molecular motor toolbox for intracellular transport. Cell. **112**, 467-480

23 Mohr, E. and Richter, D. (2001) Messenger RNA on the move: implications for cell polarity. Int. J. Biochem. Cell Biol. **33**, 669-679
24 Steward, O. and Worley, P. (2001) Localization of mRNAs at synaptic sites on dendrites. Results Probl. Cell Differ. **34**, 1-26
25 de Heredia, M. L. and Jansen, R. P. (2004) mRNA localization and the cytoskeleton. Curr. Opin. Cell Biol. **16**, 80-85
26 Mallik, R. and Gross, S. P. (2004) Molecular motors: Strategies to get along. Curr. Biol. **14**, R971-R982
27 Eom, T., Antar, L. N., Singer, R. H. and Bassell, G. J. (2003) Localization of a beta-actin messenger ribonucleoprotein complex with zipcode-binding protein modulates the density of dendritic filopodia and filopodial synapses. J. Neurosci. **23**, 10433-10444
28 Chartrand, P., Meng, X. H., Huttelmaier, S., Donato, D. and Singer, R. H. (2002) Asymmetric sorting of Ash1p in yeast results from inhibition of translation by localization elements in the mRNA. Mol. Cell. **10**, 1319-1330
29 Nicchitta, C. V., Lerner, R. S., Stephens, S. B., Dodd, R. D. and Pyhtila, B. (2005) Pathways for compartmentalizing protein synthesis in eukaryotic cells: the template-partitioning model. Biochem. Cell Biol. **83**, 687-695
30 Stephens, S. B. and Nicchitta, C. V. (2008) Divergent regulation of protein synthesis in the cytosol and endoplasmic reticulum compartments of mammalian cells. Mol. Biol. Cell. **19**, 623-632
31 Willett, M., Cowan, J. L., Vlasak, M., Coldwell, M. J. and Morley, S. J. (2009) Inhibition of mammalian target of rapamycin (mTOR) signalling in C2C12 myoblasts prevents myogenic differentiation without affecting the hyperphosphorylation of 4E-BP1. Cell. Signal. **21**, 1504-1512
32 Cowan, J. L. and Morley, S. J. (2004) The proteasome inhibitor, MG132, promotes the reprogramming of translation in C2C12 myoblasts and facilitates the association of hsp25 with the eIF4F complex. Eur. J. Biochem. **271**, 3596-3611
33 Coldwell, M. J. and Morley, S. J. (2006) Specific isoforms of translation initiation factor 4GI show differences in translational activity. Mol. Cell. Biol. **26**, 8448-8460
34 Morley, S. J. and Naegele, S. (2002) Phosphorylation of eukaryotic initiation factor (eIF) 4E is not required for de novo protein synthesis following recovery from hypertonic stress in human kidney cells. J. Biol. Chem. **277**, 32855-32859
35 Willett, M., Flint, S. A., Morley, S. J. and Pain, V. M. (2006) Compartmentalisation and localisation of the translation initiation factor (eIF) 4F complex in normally growing fibroblasts. Exp. Cell Res. **312**, 2942-2953
36 Alzhanova, D. and Hruby, D. E. (2006) A trans-golgi network resident protein, golgin-97, accumulates in viral factories and incorporates into virions during poxvirus infection. J. Virol. **80**, 11520-11527
37 Siegel, R. M., Chan, F. K., Zacharias, D. A., Swofford, R., Holmes, K. L., Tsien, R. Y. and Lenardo, M. J. (2000) Measurement of molecular interactions in living cells by fluorescence resonance energy transfer between variants of the green fluorescent protein. Sci STKE. 2000, pl1
38 Bolte, S. and Cordelieres, F. P. (2006) A guided tour into subcellular colocalization analysis in light microscopy. J. Microsc. **224**, 213-232
39 Andrade, J., Zhao, H., Titus, B., Pearce, S. T. and Barroso, M. (2004) The EF-hand Ca2+-binding protein p22 plays a role in microtubule and endoplasmic reticulum organization and dynamics with distinct Ca2+-binding requirements. Mol. Biol. Cell. **15**, 481-496
40 Yamamoto, Y., Jones, K. A., Mak, B. C., Muehlenbachs, A. and Yeung, R. S. (2002) Multicompartmental distribution of the tuberous sclerosis gene products, hamartin and tuberin. Arch. Biochem. Biophys. **404**, 210-217
41 Beuvink, I., Boulay, A., Fumagalli, S., Zilbermann, F., Ruetz, S., O'Reilly, T., Natt, F., Hall ,J., Lane, H.A., and Thomas, G. (2005) The mTOR inhibitor RAD001 sensitizes tumor cells to DNA-damaged induced apoptosis through inhibition of p21 translation. Cell. **120**, 747-59

42 Thoreen, C. C. and Sabatini, D. M. (2009) Rapamycin inhibits mTORC1, but not completely. Autophagy. **5**, 725-726
43 Robert, F., Kapp, L. D., Khan, S. N., Acker, M. G., Kolitz, S., Kazemi, S., Kaufman, R. J., Merrick, W. C., Koromilas, A. E., Lorsch, J. R. and Pelletier, J. (2006) Initiation of protein synthesis by hepatitis C virus is refractory to reduced eIF2/GTP/Met-tRNA(i) ternary complex availability. Mol. Biol. Cell. **17**, 4632-4644
44 Cao, C., Huang, X., Han, Y., Wan, Y., Birnbaumer, L., Feng, G.-S., Marshall, J., Jiang, M. and Chu, W.-M. (2009) Galpha(i1) and Galpha(i3) are required for epidermal growth factor-mediated activation of the Akt-mTORC1 pathway. Sci Signal. **2**, ra17
45 Ueda, M., Graf, R., MacWilliams, H. K., Schliwa, M. and Euteneuer, U. (1997) Centrosome positioning and directionality of cell movements. Proc. Natl. Acad. Sci. **94**, 9674-9678
46 Chicurel, M. E., Singer, R. H., Meyer, C. J. and Ingber, D. E. (1998) Integrin binding and mechanical tension induce movement of mRNA and ribosomes to focal adhesions. Nature. **392**, 730-733
47 Woods, A. J., Roberts, M. S., Choudhary, J., Barry, S. T., Mazaki, Y., Sabe, H., Morley, S. J., Critchley, D. R. and Norman, J. C. (2002) Paxillin associates with poly(A)-binding protein 1 at the dense endoplasmic reticulum and the leading edge of migrating cells. J. Biol. Chem. **277**, 6428-6437
48 Eggers, D. K., Welch, W. J. and Hansen, W. J. (1997) Complexes between nascent polypeptides and their molecular chaperones in the cytosol of mammalian cells. Mol. Biol. Cell. **8**, 1559-1573
49 Naegele, S. and Morley, S. J. (2004) Molecular cross-talk between MEK1/2 and mTOR signaling during recovery of 293 cells from hypertonic stress. J. Biol. Chem. **279**, 46023-46034
50 Svitkina, T. M., Verkhovsky, A. B. and Borisy, G. G. (1996) Plectin sidearms mediate interaction of intermediate filaments with microtubules and other components of the cytoskeleton. J. Cell Biol. **135**, 991-1007
51 Uetrecht, A. C. and Bear, J. E. (2009) Golgi polarity does not correlate with speed or persistence of freely migrating fibroblasts. Eur. J. Cell Biol. **88**, 711-7
52 Jackson, C. L. (2009) Mechanisms of transport through the Golgi complex. J. Cell Sci. **122**, 443-452
53 Marie, M., Dale, H. A., Sannerud, R. and Saraste, J. (2009) The Function of the Intermediate Compartment in pre-Golgi Trafficking Involves Its Stable Connection with the Centrosome. Mol. Biol. Cell. **20**, 4458-70
54 Osmani, N., Peglion, F., Chavrier, P., Etienne-Manneville, S (2010) Cdc42 localization and cell polarity depend on membrane traffic. J. Cell Biol. **191**, 1261-1269
55 Gomes, E. R., Jani, S. and Gundersen, G. G. (2005) Nuclear movement regulated by Cdc42, MRCK, myosin, and actin flow establishes MTOC polarization in migrating cells. Cell. **121**, 451-463
56 Polishchuk, E.V., Di Pentima, A., Luini, A., Polishchuk, R.S. (2003). Mechanism of constitutive export from the Golgi: Bulk flow via the formation, protrusion, and en bloc cleavage of large trans-golgi network tubular domains. Mol Biol Cell **14**:4470-4485.
57 Rothman, J. E. (2002) Lasker Basic Medical Research Award. The machinery and principles of vesicle transport in the cell. Nat Med. **8**, 1059-1062
58 Bonifacino, J. S. and Lippincott-Schwartz, J. (2003) Opinion - Coat proteins: shaping membrane transport. Nat. Rev. Mol. Cell Biol. **4**, 409-414
59 Drenan, R. M., Liu, X. Y., Bertram, P. G. and Zheng, X. F. S. (2004) FKBP12-rapamycin-associated protein or mammalian target of rapamycin (FRAP/mTOR) localization in the endoplasmic reticulum and the Golgi. J. Biol. Chem. **279**, 772-778
60 Wienecke, R., Maize, J. C., Jr., Shoarinejad, F., Vass, W. C., Reed, J., Bonifacino, J. S., Resau, J. H., de Gunzburg, J., Yeung, R. S. and DeClue, J. E. (1996) Co-localization of the TSC2 product tuberin with its target Rap1 in the Golgi apparatus. Oncogene. **13**, 913-923
61 Takahashi, K., Nakagawa, M., Young, S. G. and Yamanaka, S. (2005) Differential membrane localization of ERas and Rheb, two Ras-related proteins involved in the phosphatidylinositol 3-kinase/mTOR pathway. J. Biol. Chem. **280**, 32768-32774

62 Sancak, Y., Bar-Peled, L., Zoncu, R., Markhard, A. L., Nada, S. and Sabatini, D. M. Ragulator-Rag complex targets mTORC1 to the lysosomal surface and is necessary for its activation by amino acids. Cell. **141**, 290-303
63 Ma, X. M. and Blenis, J. (2009) Molecular mechanisms of mTOR-mediated translational control. Nat Rev Mol Cell Biol. **10**, 307-318
64 Liu, X. and Zheng, X. F. S. (2007) Endoplasmic Reticulum and Golgi Localization Sequences for Mammalian Target of Rapamycin. Mol. Biol. Cell. **18**, 1073-1082
65 Jones, K. A., Jiang, X., Yamamoto, Y. and Yeung, R. S. (2004) Tuberin is a component of lipid rafts and mediates caveolin-1 localization: role of TSC2 in post-Golgi transport. Exp Cell Res. **295**, 512-524
66 Buerger, C., DeVries, B. and Stambolic, V. (2006) Localization of Rheb to the endomembrane is critical for its signaling function. Biochem. Biophys. Res. Commun. **344**, 869-880
67 Sancak, Y., Peterson, T. R., Shaul, Y. D., Lindquist, R. A., Thoreen, C. C., Bar-Peled, L. and Sabatini, D. M. (2008) The Rag GTPases bind raptor and mediate amino acid signaling to mTORC1. Science. **320**, 1496-1501.

Biochemical Journal Immediate Publication. Published on 04 May 2011 as manuscript BJ20110435



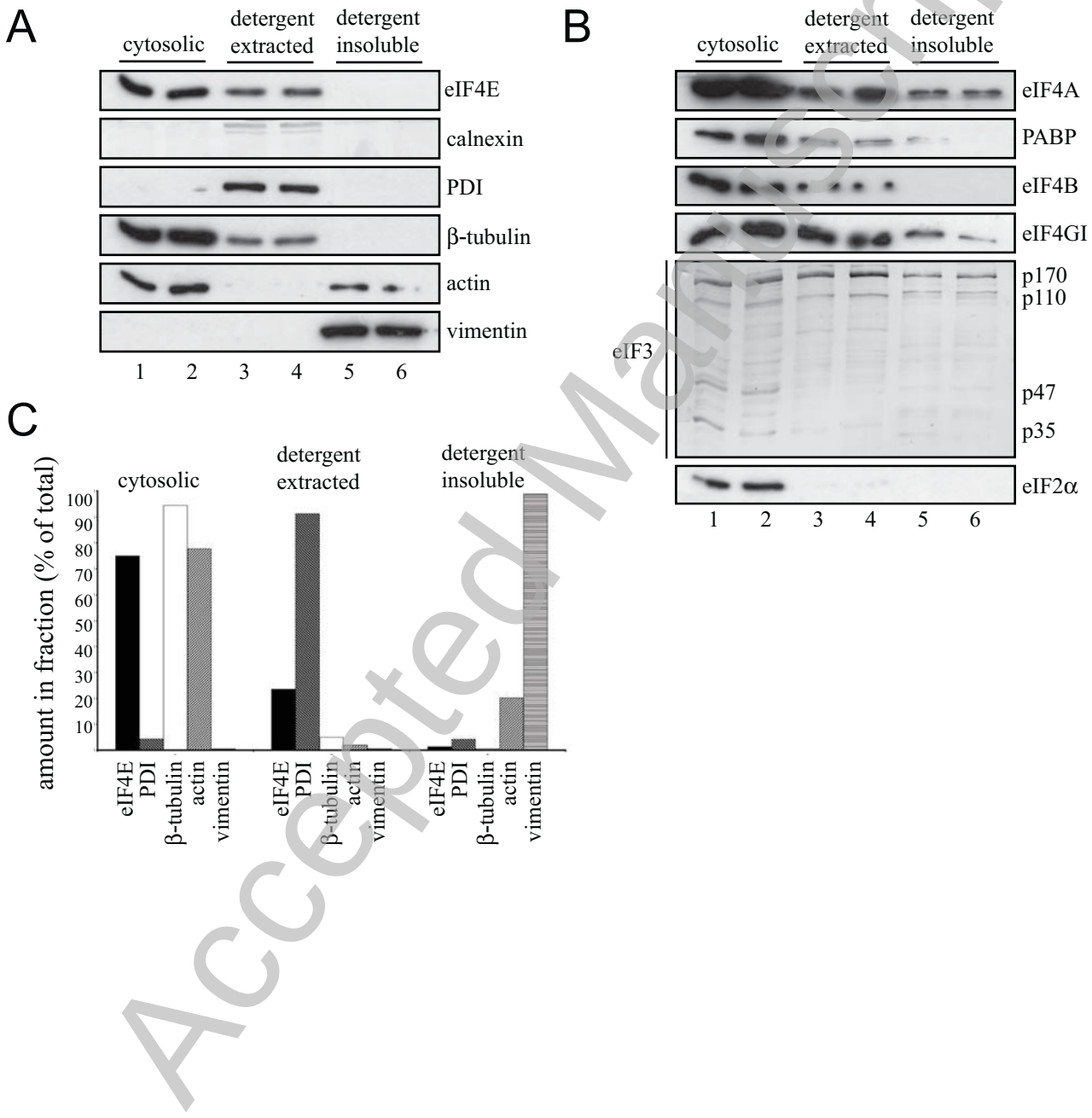

Biochemical Journal Immediate Publication. Published on 04 May 2011 as manuscript BJ20110435



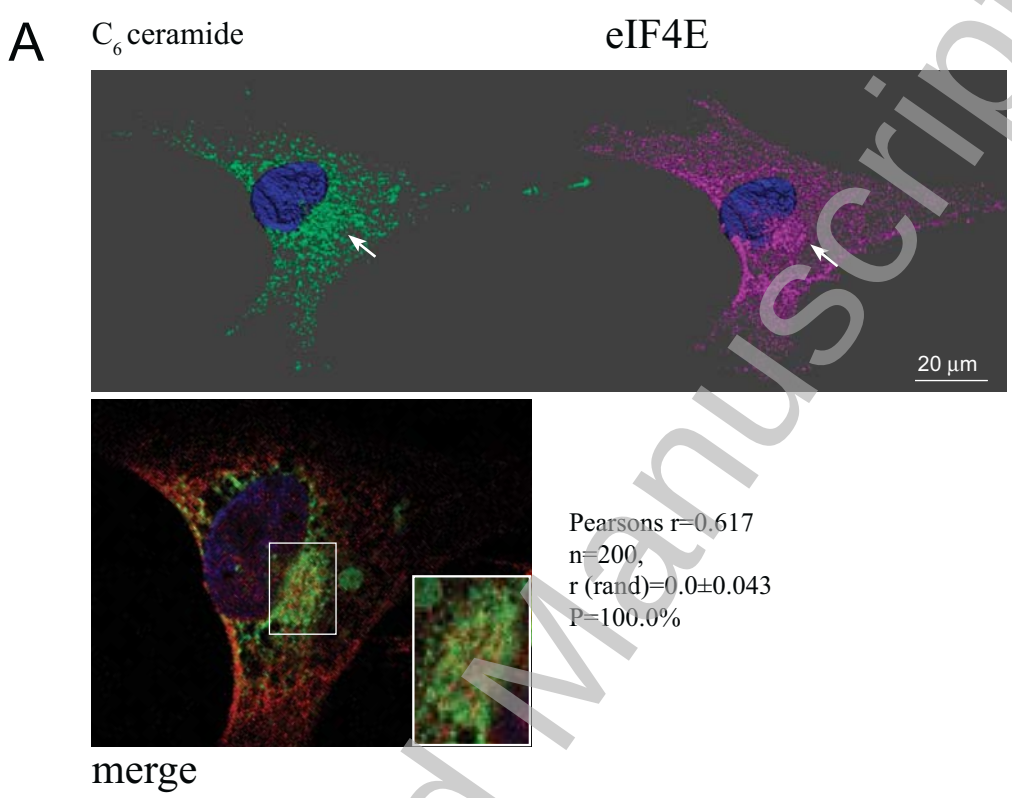

Biochemical Journal Immediate Publication. Published on 04 May 2011 as manuscript BJ20110435





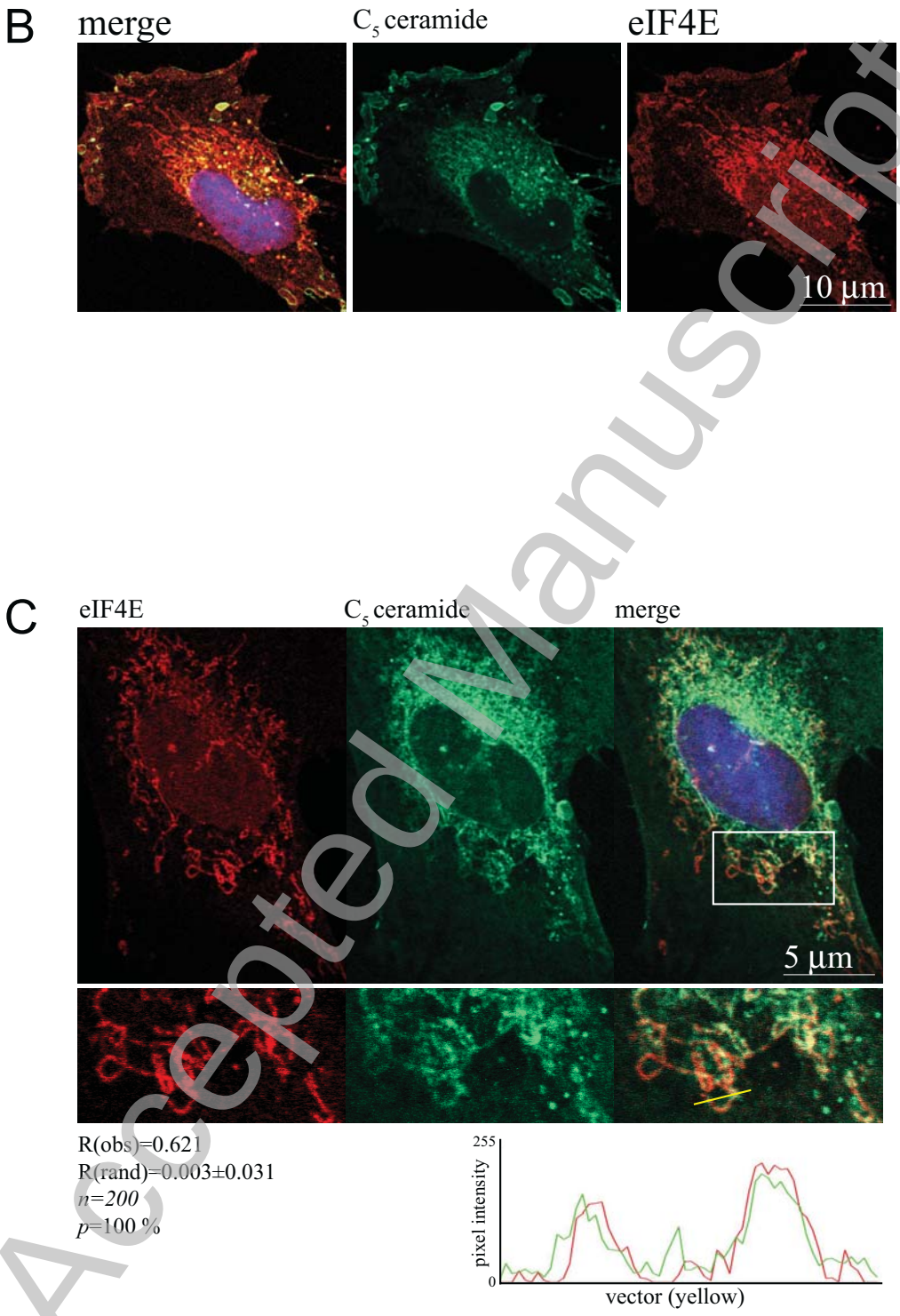

Biochemical Journal Immediate Publication. Published on 04 May 2011 as manuscript BJ20110435



D

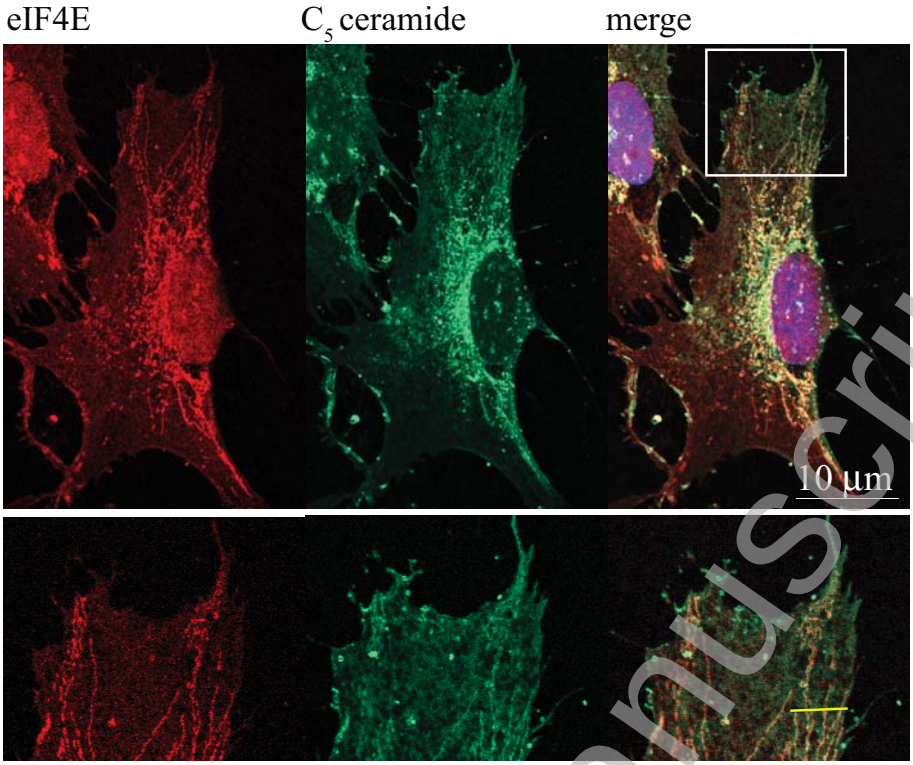


E

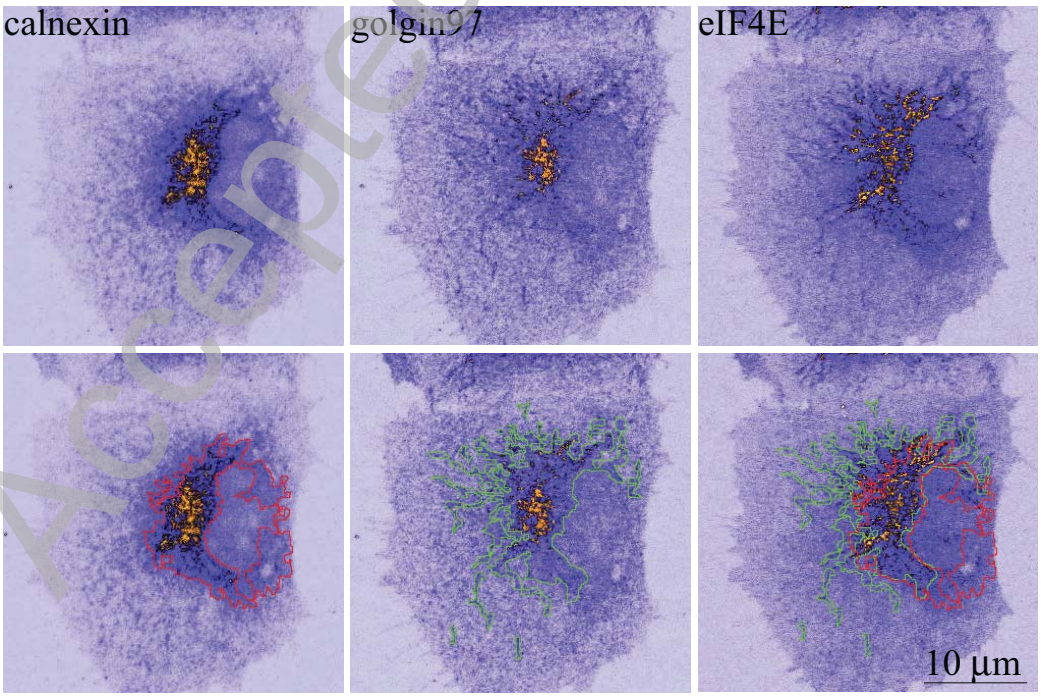

Biochemical Journal Immediate Publication. Published on 04 May 2011 as manuscript BJ20110435

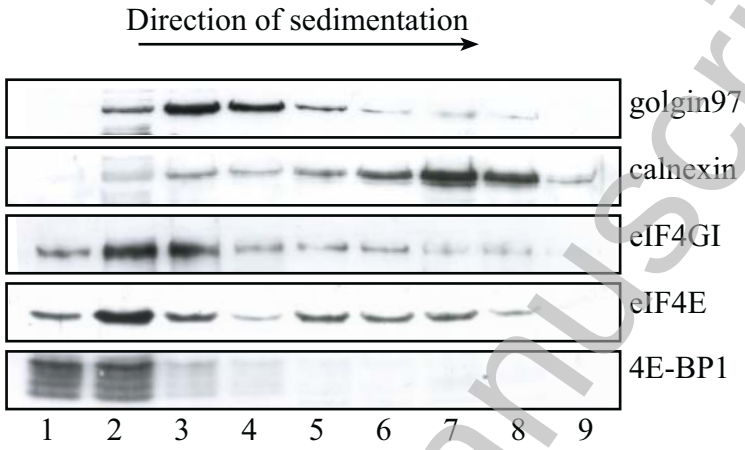

Biochemical Journal Immediate Publication. Published on 04 May 2011 as manuscript BJ20110435

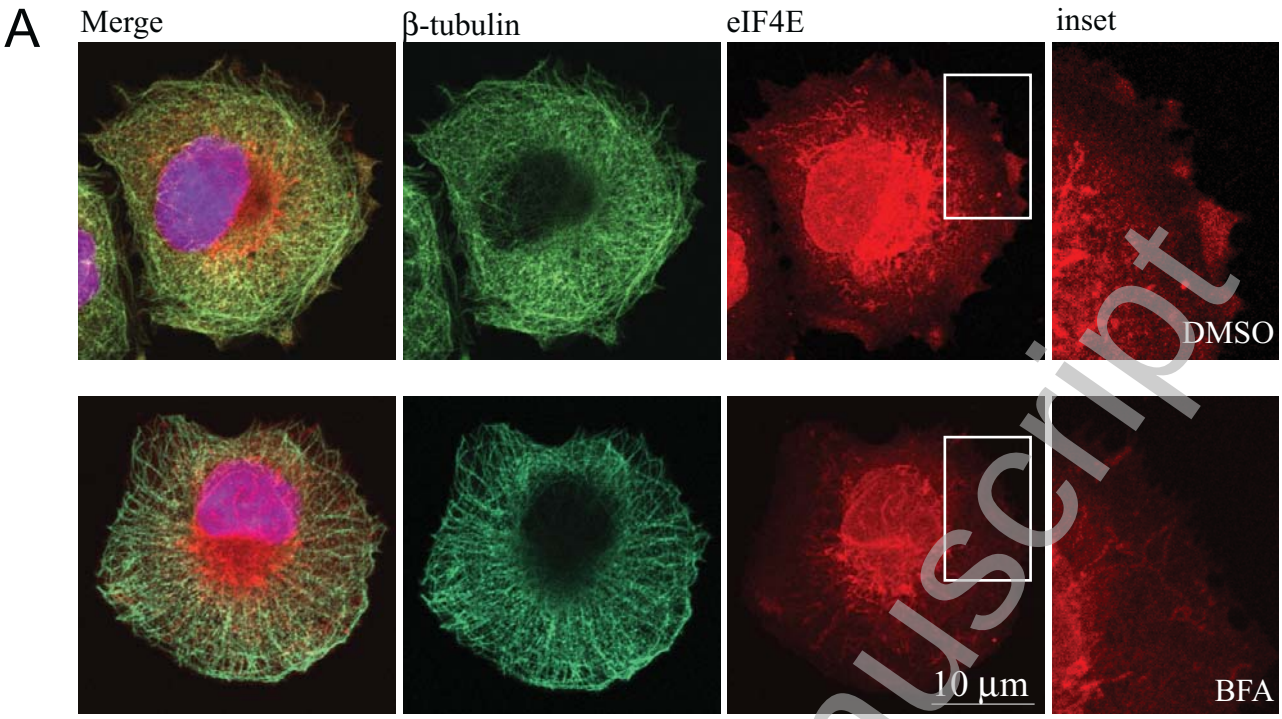


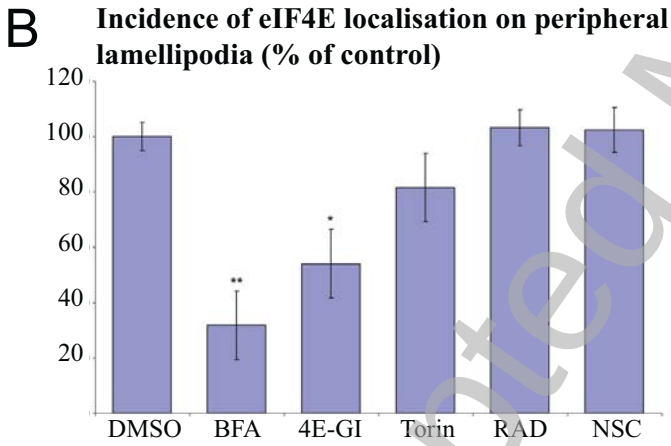


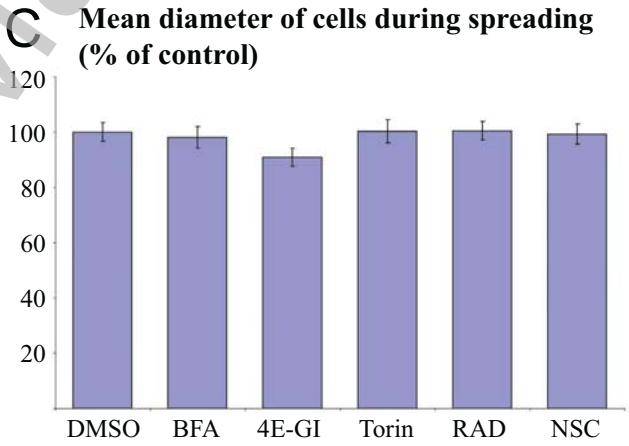

Biochemical Journal Immediate Publication. Published on 04 May 2011 as manuscript BJ20110435





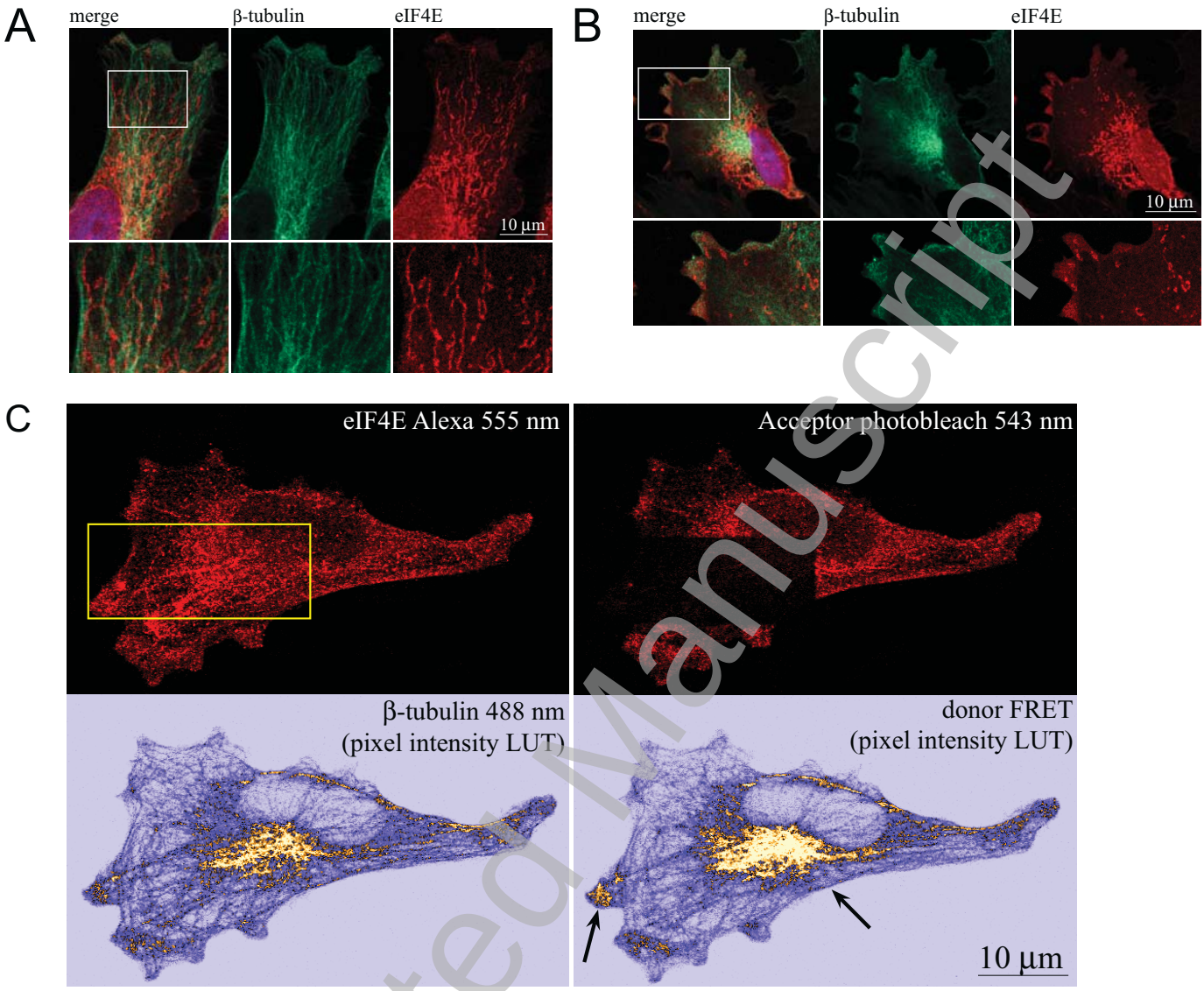

Biochemical Journal Immediate Publication. Published on 04 May 2011 as manuscript BJ20110435



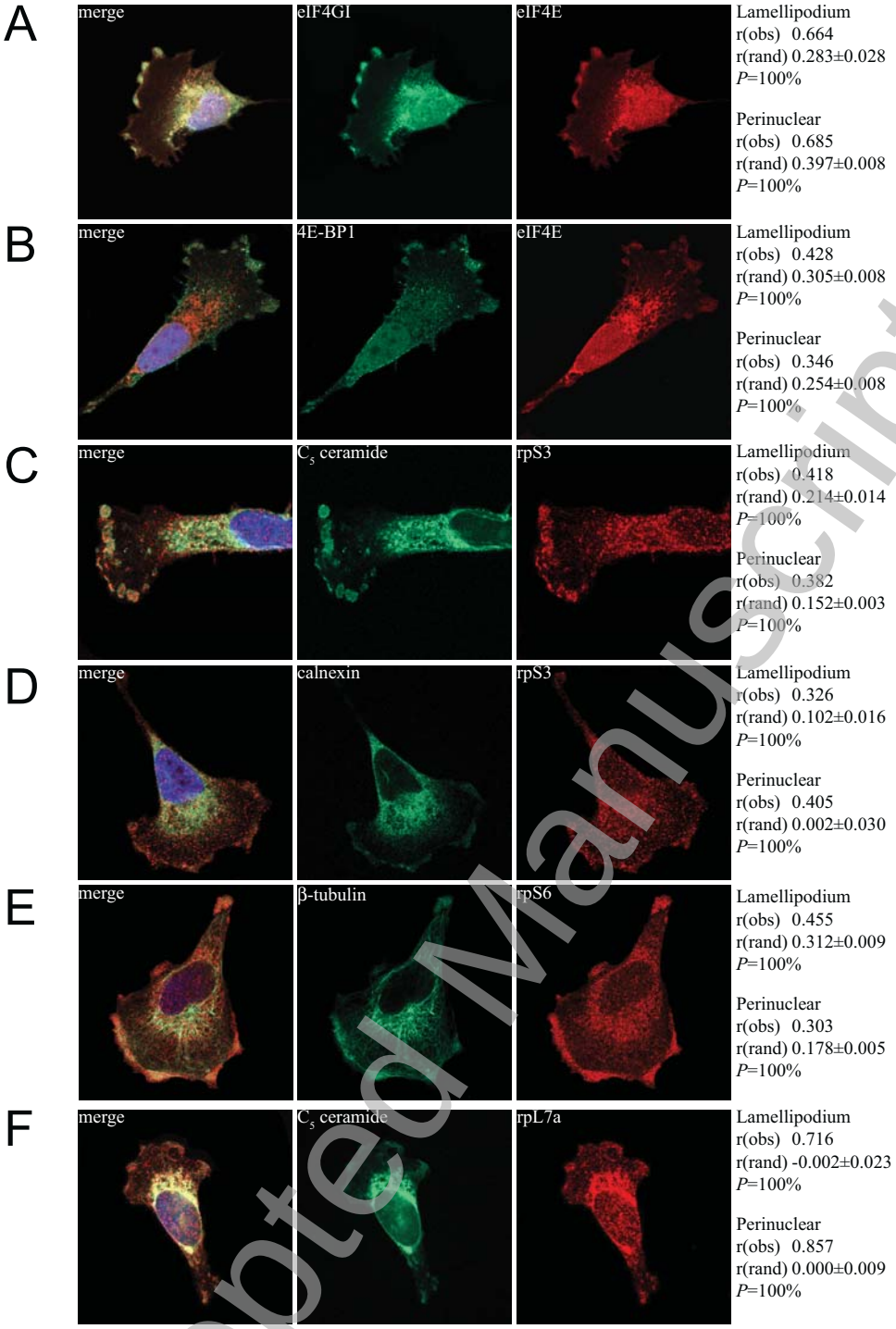

Biochemical Journal Immediate Publication. Published on 04 May 2011 as manuscript BJ20110435